

Article

ADHD symptoms map onto noise-driven structure-function decoupling between hub and peripheral brain regions

Luke J. Hearne^{1§}, Hsiang-Yuan Lin^{2§}, Paula Sanz-Leon³, Wen-Yih Isaac Tseng^{4,5}, Susan Shur-Fen Gau^{2,5*}, James A. Roberts³, Luca Cocchi¹

¹ Clinical Brain Networks Group, QIMR Berghofer Medical Research Institute, Brisbane, Queensland, Australia

² Department of Psychiatry, National Taiwan University Hospital, and College of Medicine, Taipei, Taiwan

³ Brain Modelling Group, QIMR Berghofer Medical Research Institute, Brisbane, Queensland, Australia

⁴ Institute of Medical Device and Imaging, National Taiwan University College of Medicine, Taipei, Taiwan

⁵ Graduate Institute of Brain and Mind Sciences, National Taiwan University College of Medicine, Taipei, Taiwan

[§]Shared first authorship

*Corresponding author:

Susan Shur-Fen Gau

Department of Psychiatry, National Taiwan University Hospital and College of Medicine
No. 7, Chung-Shan South Road, Taipei, Taiwan 10002.

Tel: +886-2-23123456 ext.66802, Fax: +886-2-23812408

Email: gaushufe@ntu.edu.tw

Abbreviated title: Brain network structure-function coupling in ADHD

Number of words: 248 (abstract), 3496 (main text), 57 references

Number of figures and tables: 3 figures and 1 table

Supplementary information: supplementary methods; 3 supplementary figures; 4 supplementary tables

Abstract

Adults with childhood-onset attention-deficit hyperactivity disorder (ADHD) show altered whole-brain connectivity. However, the relationship between structural and functional brain abnormalities, the implications for the development of life-long debilitating symptoms, and the underlying mechanisms remain uncharted. We recruited a unique sample of 80 medication-naive adults with a clinical diagnosis of childhood-onset ADHD without psychiatric comorbidities, and 123 age-, sex-, and intelligence-matched healthy controls. Structural and functional connectivity matrices were derived from diffusion spectrum imaging and multi-echo resting-state functional MRI data. Hub, feeder, and local connections were defined using diffusion data. Individual-level measures of structural connectivity and structure-function coupling were used to contrast groups and link behavior to brain abnormalities. Computational modeling was used to test possible neural mechanisms underpinning observed group differences in the structure-function coupling. Structural connectivity did not significantly differ between groups but, relative to controls, ADHD showed a reduction in structure-function coupling in feeder connections linking hubs with peripheral regions. This abnormality involved connections linking fronto-parietal control systems with sensory networks. Crucially, lower structure-function coupling was associated with higher ADHD symptoms. Results from our computational model further suggest that the observed structure-function decoupling in ADHD is driven by heterogeneity in neural noise variability across brain regions. By highlighting a neural cause of a clinically meaningful breakdown in the structure-function relationship, our work provides novel information on the nature of chronic ADHD. The current results encourage future work assessing the genetic and neurobiological underpinnings of neural noise in ADHD, particularly in brain regions encompassed by fronto-parietal systems.

Introduction

Adult attention-deficit hyperactivity disorder (ADHD) is a common neurodevelopmental disorder characterized by inattentive and hyperactive-impulsive symptoms beginning in early childhood¹. Identifying the neural underpinnings of adult ADHD is an ongoing research endeavor, critical to the definition of neural mechanisms supporting clinical outcomes of childhood-onset ADHD and the development of novel targeted interventions².

Neuroimaging work has provided important insights into altered structural³⁻⁵ and functional^{6,7} brain connectivity underpinning ADHD pathophysiology, and suggest that network interactions, rather than regional abnormalities, contribute to phenotypic expression of the disorder⁸. Anatomically, results have been mixed. Recent studies showing no changes in the ADHD connectome⁹, whereas others have pointed to various abnormalities in white matter tracts including the corpus callosum and posterior circuits related to the limbic and occipital systems, the fronto-striato-cerebellar connections, and the pathways linking the default-mode and fronto-parietal hub regions^{4,5,10}.

Complementing findings from diffusion MRI, resting-state functional magnetic resonance image (rs-fMRI) studies have highlighted that both diagnosis and symptoms of ADHD are linked to reduced segregation between the activity of control networks supporting external task engagement and the default-mode network^{6,7,11}. Reduced functional connectivity within, and between, the default-mode, sensory, and control networks has also been reported both in children and adults with ADHD^{6,7,10,11}.

Emerging evidence suggests that patterns of functional connectivity are constrained by their anatomical underpinning: The connectome^{12,13}. Structural and functional brain network alterations in adult ADHD partially overlap, but the direct link between these structure-function aberrations has not been formally explored. Here, we used multi-echo rs-fMRI and diffusion spectrum imaging (DSI) to investigate possible changes in whole-brain structure-function coupling in a large sample of well-characterized, medication-naïve adults with childhood-onset ADHD and matched healthy controls¹¹. Based on previous findings¹¹ and the hypothesis that psychiatric conditions are primarily pathologies of brain hubs¹⁴, we expected significant departures from the typical structure-function coupling in ADHD. Specifically, a breakdown in the structure-function association is likely to occur in connections involving brain hubs that belong to the control and default-mode brain networks^{14,15}. To investigate a likely underlying neural mechanism of this deficit¹⁶, we adopted whole-brain computational modeling. Our model explicitly tested the hypothesis that increased heteroscedasticity in the levels of intrinsic neural noise drives the expected breakdown in the structure-function coupling. Heteroscedasticity occurs when the variance of explanatory variables – neural noise level – is not constant across brain regions. The hypothesis tested by our model is grounded in previous work suggesting that ADHD symptoms are linked to a pathological increase in baseline neural noise¹⁷⁻²⁰.

Methods

Sample

We recruited 80 medication-naïve adults with childhood-onset ADHD aged 18–39 years (mean 26.7 years), who fulfilled DSM-IV-TR criteria for the current diagnosis of ADHD. This carefully phenotyped sample allows the unequivocal assessment of structural and functional brain networks in the absence of common confounds in ADHD research including other developmental delays, medication exposure and intellectual disabilities. Results from the clinical sample were benchmarked against the findings of 123 age-, sex-, and IQ-matched healthy controls. Participants were assessed at the Department of Psychiatry, National Taiwan University Hospital (NTUH), Taipei, Taiwan.

This study has been approved by the Research Ethics Committee of NTUH (201401024RINC; ClinicalTrials.gov number: NCT02642068) and all participants provided written informed consent. Details regarding the recruitment procedure are described in our previous work¹¹ (**Supplementary Methods**).

MRI acquisition and preprocessing

Brain imaging data were acquired with a Siemens 3T Tim Trio scanner equipped with a 32-channel head coil. Details regarding preprocessing multi-echo resting-state data are described elsewhere¹¹ (**Supplementary Methods**). In short, the pipeline included: quality control, comprehensive data denoising using multi-echo independent components analysis (ME-ICA v3.0)²¹, coregistration to individual anatomical images, non-linear normalization to MNI space, and filtering (0.01~0.1 Hz).

DSI data underwent an initial quality control procedure to ensure acceptable levels of in-scanner head motion, which were estimated by signal loss²². This quality control step resulted in a final sample of 78 ADHD adults and 118 healthy controls (**Table 1**). DSI data were then reconstructed using the q -space diffeomorphic reconstruction approach²³ implemented in the software DSI Studio (**Supplementary Methods**).

Further quality control analyses showed that micro-head movements (mean framewise displacement)²⁴ for rs-fMRI and signal dropout counts²² for DSI, were not significantly different between ADHD and controls ($p = 0.35$ and 0.54 , respectively).

Table 1. Demographic and clinical features of the participants.

Mean (SD)	Control (N=118)	ADHD (N=78)	Statistics
Age (18-39 years)	25.8 (5.0)	26.6 (5.5)	$p = 0.287$
Sex (M/F)	76/42	54/24	$p = 0.484$
FIQ	109.8 (9.3) (range: 89-138)	107.5 (10.4) (range: 80-137)	$p = 0.101$
VIQ	108.2 (9.0)	105.7 (11.2)	$p = 0.088$
PIQ	110.4 (11.4)	108.3 (16.3)	$p = 0.289$
ADHD symptoms			
SNAP-IV (Parent-report)^a			
Inattention (0-27)	6.6 (4.9)	19.6 (5.0)	$p < 0.001$
Hyperactivity/Impulsivity (0-27)	3.2 (4.4)	13.4 (6.4)	$p < 0.001$
ASRS (Self-report)			
Inattention (0-36)	13.3 (5.2)	27.0 (4.8)	$p < 0.001$
Hyperactivity/Impulsivity (0-36)	9.1 (5.2)	19.9 (6.3)	$p < 0.001$
Mean frame-wise displacement^b (mm)	0.045 (0.021) (range: 0.014-0.123)	0.048 (0.024) (range: 0.017-0.108)	$p = 0.354$
Signal dropout counts^c	30.8 (22.4)	28.8 (21.4)	$p = 0.536$

^a Measured by the parent-rated Swanson, Nolan, and Pelham, version IV (SNAP-IV) scale.

^b A summary estimate of in-scanner motion levels of resting-state fMRI, as estimated by the Euclidian norm (enorm: square root of the sum of squares of the differences in motion derivatives), computed with AFNI's `1d_tool.py`.

^c A summary estimate of in-scanner motion levels of diffusion spectrum imaging (see the Methods).

Abbreviation: ADHD=attention-deficit hyperactivity disorder; FIQ=full intelligence quotient; PIQ=performance intelligence quotient; VIQ=verbal intelligence quotient; ASRS=Adult ADHD Self-Report Scale; M=male; F=female; R=right; L=left; SD=standard deviation.

Structural and functional brain network construction

We generated whole-brain structural (SC) and functional (FC) connectivity matrices for each individual, based on a common and recently validated cortical parcellation²⁵ (**Fig. 1A**). Fourteen additional subcortical structures from the Harvard-Oxford atlas were added to the parcellation, resulting in 214 total regions (*Schaefer-214* henceforth; **Supplementary Table 1**). Individual whole-brain tractography maps were combined with the pre-defined anatomical boundaries defined by this *Schaefer-214* parcellation to generate a weighted SC matrix (**Fig. 1B**). Each edge of the network corresponds to the total number of normalized streamlines that interconnect any two brain regions, adjusted for the interregional fiber length²⁶. For resting-state data, regional time-series were calculated as the mean across voxels within each region included in the brain parcellation. For each individual, Pearson's correlations were calculated between the time-series of all regions to calculate FC. Finally, a Fisher z-transformation was applied to the FC matrices.

Connection classes

We identified hub regions according to an aggregate ranking across multiple metrics including degree, strength, subgraph centrality, and betweenness^{27,28}. The top 15% composite scores ($N = 32$, **Supplementary Table 1&2**) were used to identify hub regions within each individual; all other nodes were assigned as *periphery* nodes. Hub *connections* were defined as edges that connected any two hub nodes. Feeder connections linked hub nodes to periphery nodes, and local connections linked periphery nodes (**Fig. 1C**)^{15,29}.

Structure-function relationships

Brain network structure-function relationships were conducted in line with previous research¹⁵. First, non-zero SC values within each individual connectome were isolated and normalized using a rank-based inverse Gaussian transformation³⁰. The resulting SC values were correlated with corresponding FC values (i.e., the same edges), within each individual. This analysis produced a single Pearson's r value that summarized the global structure-function association for each individual³¹. These values were used to populate group distributions and were subsequently contrasted using between-group statistics. This entire procedure was completed at the level of the whole network and within each respective connection class: hubs, feeders, and local edges.

Previous work investigating resting-state networks, including data from the current cohort¹¹, has highlighted the key role of control, default-mode, and sensory networks in adult ADHD^{6,7}. Based on these results, we also tested for specific changes in SC-FC coupling within these networks. To ensure that a sufficient number (minimum of 50) of edges was used to infer structure-function relationship, control networks were defined as the combination of fronto-parietal, alongside dorsal and ventral attention affiliations from the adopted parcellation, while sensory connections included both visual and somatomotor affiliations. Default-mode connections were as in the original parcellation. Once SC-FC coupling was estimated within each network, the mean r values (Control-ADHD) were presented within and between each network.

Relationship between structure-function coupling and behavioral symptoms of ADHD

Given the notion that measures of ADHD symptoms are continuously distributed in the general population^{32,33}, we investigated brain-behavior relationships across both ADHD and control groups (**Fig. 1C**). Inattention and hyperactivity-impulsivity symptoms based on the parent-rated Swanson, Nolan, and Pelham, IV (SNAP-IV)³⁴ and self-rated Adult ADHD Self-Report Scale (ASRS)³⁵ (**Table 1**) were used in the analysis. These four symptom items (two from each measure) were transformed using a rank-based inverse Gaussian, then entered into a principal component analysis to reduce the dimensionality of the data. The first component, accounting for 81% of the variance, was then correlated with the structure-function coupling of the whole sample (**Supplementary Table 3**).

Statistical comparisons between groups

To ensure that the general structural network density did not explain between-group differences, summed binary and weighted degrees were compared between groups. Average connection weights within each *connection class* were compared between each group. In addition, the network based statistic (NBS)³⁶ was used to explore any possible differences in SC between controls and ADHD (5000 permutations, threshold $t = 3$). ADHD-associated alterations of FC using NBS have been reported in our initial study on this sample¹¹.

Mann–Whitney U tests were used to identify possible differences in the structure-function association between control and ADHD groups. Bonferroni correction (family-wise error rate, FWE) for multiple comparisons was applied to follow-up statistics, with $\alpha_{FWE} < 0.05$ indicating statistical significance. Statistical analyses were performed in MATLAB (Mathworks) with code available online (<https://github.com/ljhearme/ADHDSCFC>).

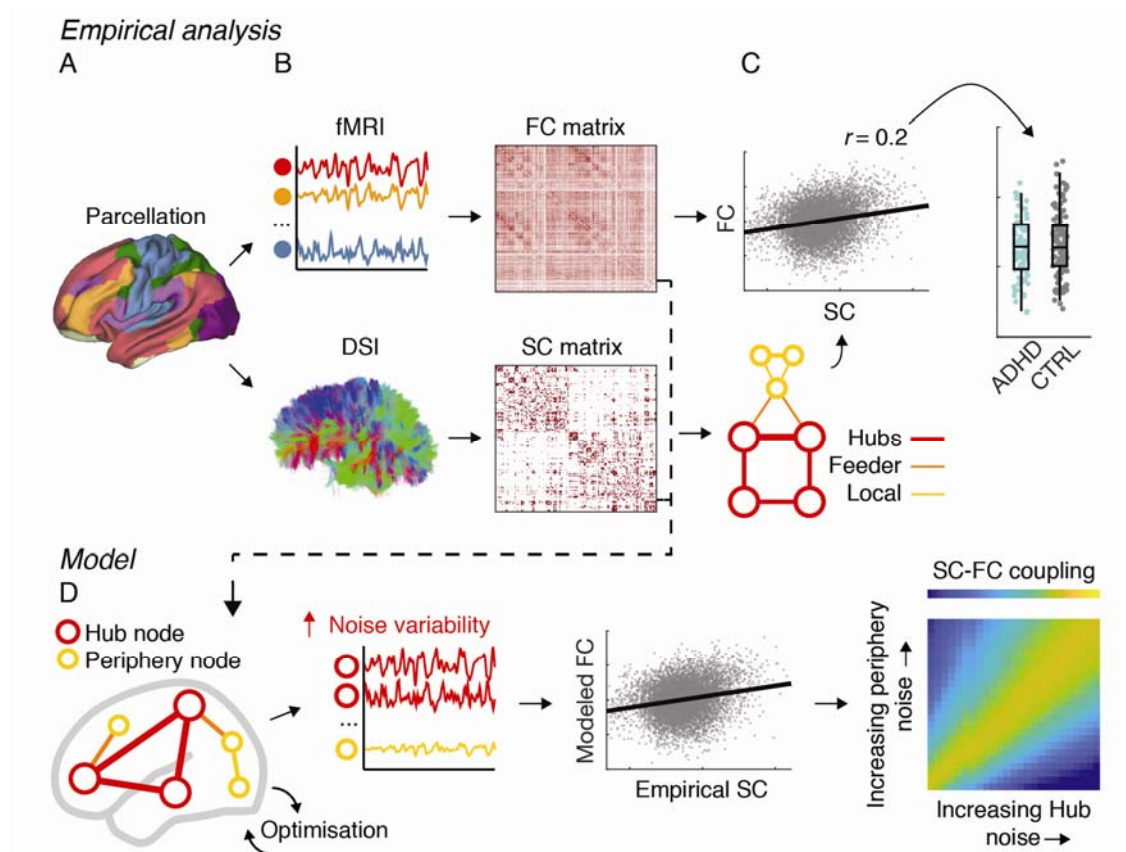


Fig. 1 Conceptual overview of the analysis pipeline. **A.** Analyses were conducted using a whole-brain parcellation including 214 cortical and subcortical regions. Replication analyses were performed using two alternative brain parcellations (see text). **B.** Structural (SC) and functional connectivity (FC) matrices were derived from diffusion spectrum imaging (DSI) and multi-echo resting-state fMRI data, respectively. Darker colors indicate higher normalized streamline counts (SC) and higher Fisher-z normalized Pearson’s correlation values between every possible pair of brain regions (FC). **C.** The

topological organization of the SC matrices was examined to derive measures of different connection types: hub connections, feeder connections, and local connections. Individual-level correlations between SC and FC were used to estimate structure-function coupling, which was then analyzed with between-group statistics. **D.** A computational model was used to assess the potential neural mechanisms that lead to decreased structure-function coupling. Empirical SC was used as input in the model and model parameters were estimated by fitting to empirical FC. We systematically assessed if an increase in the noise heterogeneity in hub or peripheral nodes could result in a marked dissociation between functional and structural connectivity.

Computational modeling: Assessing the neural factors driving structure-function breakdown

The adopted whole-brain computational model incorporates SC to represent the strength of connections between brain regions. In addition to the weights specified in the empirical SC matrix, structural connections are scaled by a global coupling parameter. This parameter can then be varied systematically to simulate and compare the global dynamics emerging from the model with the empirical FC derived from the rs-fMRI data.

We chose a simple stochastic linear model of the Ornstein-Uhlenbeck type^{37–39}. The main motivations behind this choice were that the model: (i) allows us to simulate whole-brain patterns of FC *from* SC matrices; (ii) enables tests of the hypothesis that increased heteroscedasticity of neural noise levels results in a breakdown in structure-function coupling; (iii) can be considered a generic linearization of more complex models with a stable fixed point (a mathematical approach at the core of e.g. dynamic causal modeling for fMRI⁴⁰); and (iv) permits a direct analytical derivation of FC from empirical SC without the need of computationally demanding numerical simulations. The model equation is:

$$dx_i = \left(-x_i + c \sum_{j=1}^N W_{ij} x_j \right) dt + \sigma_i dW_i$$

where x_i is the activity of the i -th region; c is the global coupling strength which rescales the strength of structural connections of the system; W_{ij} is the connectivity weight to region i from region j (as specified by the empirical SC matrix); σ_i is the intrinsic noise amplitude/level of the i -th region, and defines the size of random increments $\sigma_i dW_i$ in the dynamics of the region, and N is the total number of regions in the connectome. Previous modeling studies^{38,39} have considered the noise levels to be constant across the whole network (i.e., the homoscedastic case in which all σ_i are identical). In light of previous suggestions^{17–20}, we hypothesized that heteroscedasticity across a specific subset of brain regions (hubs or periphery) would have a detrimental impact on SC-FC decoupling. To test our hypothesis and determine in which connection classes heteroscedasticity has the largest impact, we systematically analyzed varying degrees of heteroscedasticity in the noise levels in distinct subsets of regions independently (hub and periphery regions). A comprehensive description of the modeling can be found in the **Supplementary Methods**.

Results

Similar structural connectivity between groups

Results showed no difference in weighted ($p = 0.89$, $z = 0.13$), or unweighted ($p = 0.24$, $z = -1.19$) summed degree across groups. Likewise, the whole-brain network-based statistics comparing ADHD and healthy control groups revealed no significant differences in structural connectivity between the groups (ADHD > controls, $p = 0.63$; controls > ADHD, $p = 0.78$). Next, we sought to investigate potential differences in *classes* of structural connections, namely hubs, feeders, and local connections. No significant group differences were observed when comparing mean connection strength within hub ($p = 0.86$, $z = -0.17$), feeder ($p = 0.77$, $z = -0.29$), or local connections ($p = 0.23$, $z = 1.21$).

Structure and function coupling in ADHD is reduced in feeder connections

When considering all edges within the network, results indicated a significant difference in SC-FC coupling ($p = 0.01$, $z = 2.51$, **Fig. 2A**). We then assessed the contribution to this effect of each connection class (hub, feeder or local). Results showed that compared to controls, ADHD had a significantly lower SC-FC association in feeder connections ($p_{FWE} = 0.005$, $z = 3.10$) but not in hub ($p_{FWE} = 1$, $z = 0.55$) or local ($p_{FWE} = 0.33$, $z = 1.60$) connections (**Fig. 2A**).

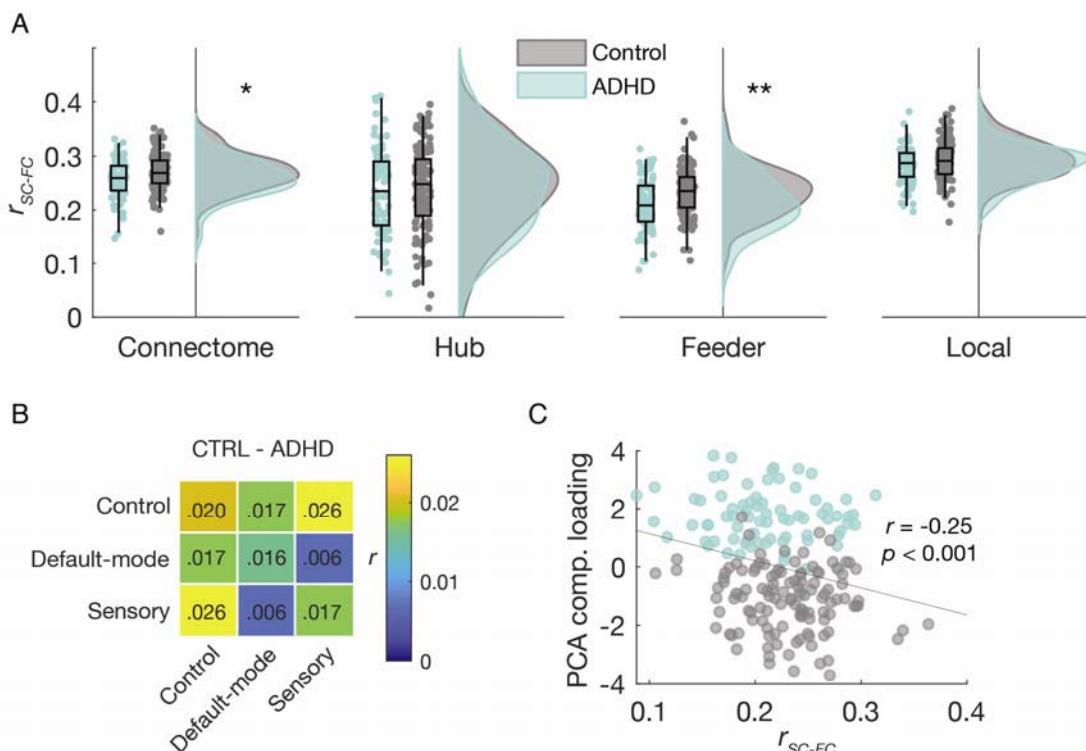


Fig. 2 Structure-function relationships in drug-naïve adults with ADHD and healthy matched controls. **A**. Distributions of r values across the whole connectome and the three connection classes⁵⁷. Significant differences between ADHD and Control groups were observed in the whole connectome

but were driven by a large group difference in feeder connections. **B.** Mean differences in SC-FC coupling (Controls *minus* ADHD) when constrained to feeder connections within and between control, default-mode, and sensory functional networks. The largest deficit in SC-FC coupling in ADHD compared to controls were found between control and sensory network connections ($r = 0.026$). **C.** Correlation between symptoms and SC-FC coupling in feeder connections. SC-FC coupling strength was negatively correlated with the ADHD symptom factor scores derived from principal components analysis. * < 0.05 , ** < 0.01 corrected for multiple comparisons.

Feeder structure-function decoupling in control, default-mode, and sensory brain networks

To further explore the anatomical specificity of the observed deficits in structure-function coupling, we isolated feeder connections that belonged to control, default-mode, or sensory (merging somatomotor and visual) networks. As per the previous analysis, we correlated SC and FC values for connections within and between the selected brain networks. This resulted in a three-by-three matrix for both ADHD and healthy control groups that represented the degree of SC-FC coupling within and between control, default mode, and sensory networks. The largest reduction in SC-FC associations in ADHD compared to healthy controls were located in connections between control and sensory networks (**Fig. 2B**).

The magnitude of structure-function decoupling correlates with the severity of ADHD symptoms

Individual symptom scores captured by PCA linearly correlated with indices of structure-function coupling in feeder connections, such that lower structure-function coupling was associated with more severe ADHD symptoms ($p = 0.0004$, $r = -0.25$, **Fig. 2C**).

Control analyses

A number of tests were conducted to establish the reliability of our findings. To ensure that our chosen brain parcellation had little bearing on the results⁴¹, we repeated the analyses in two other, independent brain parcellations: *Shen-213*⁴² and *Brainnetome-244*⁴³. The reported effects were all successfully replicated (**Supplementary Table 2**). Using these alternative brain parcellations, we also found that adults with ADHD exhibited weaker structure-function coupling in hub connections. However, the effect size of these between-group differences was consistently smaller than the effect in feeder connections.

Noise in hubs and periphery as a neural mechanism for structure-function breakdown

Finally, we sought a neural mechanism for how altered structure-function relationships could emerge in the absence of significant differences in the connectome. In particular, we aimed to use computational modeling to explain our finding of selective deficits in feeder connection SC-FC coupling (leaving hub and local connections relatively unscathed). We systematically explored two scenarios with noise heteroscedasticity – i.e., increased heterogeneity in the intrinsic neural noise levels σ_i across brain regions.

In the first scenario, we analyzed the simple case of heterogeneity between hubs and periphery ($\sigma_H \neq \sigma_P$) for hub nodes (H) and peripheral regions (P), maintaining σ_H and σ_P constant *within* each class of regions. Exploring ranges of σ_H and σ_P (**Fig. 3A-C**) we analyzed the changes in SC-FC coupling for the three classes of connections (hub, feeder, and local). We found that feeder connections were the most susceptible to subtle imbalances between intrinsic noise levels in hub and periphery regions, reflected in the quick decrease in SC-FC coupling (**Fig. 3B**). On the contrary, hub and local connections exhibited only small changes (**Fig. 3A&C**). Specifically, a small imbalance such that $\sigma_H < \sigma_P$, with σ_P 10% larger than σ_H , produced a slight ($< 2\%$) reduction in SC-FC coupling in hubs compared to the homogenous $\sigma_H = \sigma_P$ case, similar to the empirically observed slight decrease for hub connections in **Fig. 2A** ($< 2\%$). Conversely, a 10% imbalance in the opposite direction ($\sigma_H > \sigma_P$) yielded a negligible ($\sim 0.3\%$) increase in hub SC-FC coupling. The increased sensitivity of feeder connections was demonstrated by the same 10% imbalance ($\sigma_H < \sigma_P$) resulting in a 4% decrease in SC-FC coupling for feeder connections compared to the homogenous case. Importantly, an imbalance of approximately 50% ($\sigma_H < \sigma_P$) was required to obtain the 10% decrease in SC-FC coupling empirically observed in ADHD feeder connections (**Fig. 2A**). This larger imbalance also resulted in a $< 2\%$ reduced SC-FC coupling in hub connections, again in accordance with empirical results. Thus, larger differences between mean noise amplitude levels in hubs and periphery led to greater SC-FC decoupling specific to feeder connections, mirroring the selective deficits observed in ADHD.

In the second scenario, we modeled the more realistic case where the noise levels (σ_i) within hubs and periphery also varied from region to region. This allowed us to examine whether heteroscedasticity within hubs and/or periphery regions could contribute to the observed disruption of SC-FC coupling in ADHD. We systematically explored ranges of variance ($\text{Var}[\sigma_H]$ and $\text{Var}[\sigma_P]$) for noise levels normally distributed around means ($E[\sigma_H]$ and $E[\sigma_P]$), set here such that $E[\sigma_P]$ is 10% larger than $E[\sigma_H]$ in line with the above results for hub connections (comparing **Fig. 3A** to **Fig. 2A**). We found that connections within a region class (i.e., hub-hub or periphery-periphery) are resilient to increased variability of intrinsic noise levels in the opposite type. Indeed, the SC-FC coupling in hub connections (**Fig. 3D**) and local connections (**Fig. 3F**) remained almost constant for increased noise variability in peripheral and hub regions, respectively. However, feeder connections (**Fig. 3E**) are clearly susceptible to changes in noise level heterogeneity within either hub or periphery regions, which implies an increased sensitivity to heteroscedasticity could also contribute to the disruption of SC-FC coupling in ADHD.

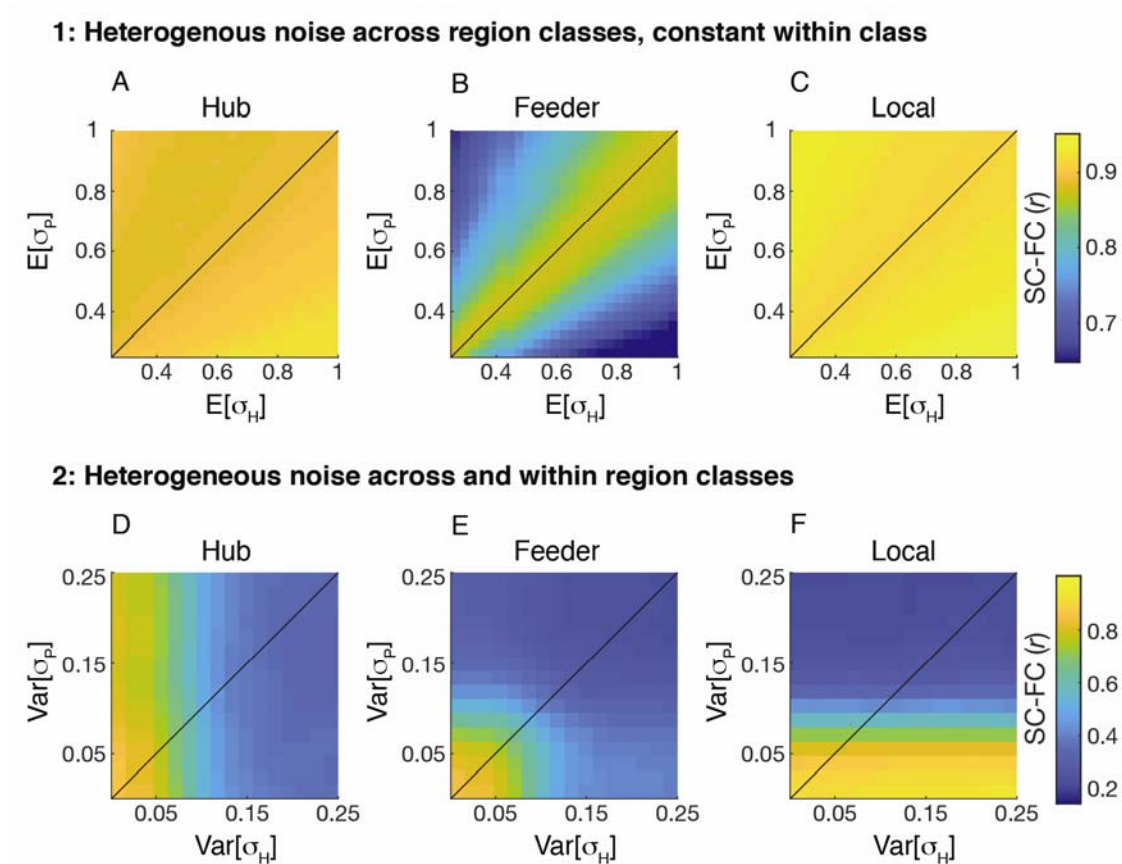


Fig. 3 Modeling the effect of noise heteroscedasticity on structure-function coupling. Effects of noise heteroscedasticity on SC-FC coupling. *Top row*: Scenario 1 - Noise heterogeneity between hubs and periphery ($\sigma_H \neq \sigma_P$) for hubs (H) and peripheral brain regions (P), σ_H and σ_P constant within each class of regions (hubs and periphery). *Bottom row*: Scenario 2 - noise levels (σ_i) within hubs and periphery varied from region to region. The colormaps quantify the SC-FC coupling (Pearson correlation between SC and FC matrix entries). **A/D**. Hub connections. **B/E**. Feeder connections. **C/F**. Local connections. $E[\cdot]$ = expected mean value; $\text{Var}[\cdot]$ = variance. The line in each panel corresponds to the case $E[\sigma_H] = E[\sigma_P]$ (top row) or $\text{Var}[\sigma_H] = \text{Var}[\sigma_P]$ (bottom row).

Discussion

The present study provides evidence of a clinically significant breakdown in brain structure-function (SC-FC) coupling in medication-naïve adults with childhood-onset ADHD. In line with the hypothesis that hub regions are critically vulnerable to brain pathology^{14,15,44}, ADHD was associated with a marked SC-FC decoupling in connections linking brain hubs to peripheral regions (feeders) within and between control and sensory networks. Results from our modeling work further suggest that such decoupling could be linked to: (i) an imbalance in noise amplitudes in hubs and the periphery (e.g., increased 'unreliability' in signals originating from the periphery) and, (ii) higher peripheral heteroscedasticity (i.e., the peripheral noise is more diverse and more difficult for the hubs to filter out). Altogether,

results from this work propose a novel neural mechanism explaining structure-function decoupling in brain connectivity underpinning the chronic manifestation of ADHD symptoms.

Structural networks are thought to place significant constraints on FC and local brain activity^{12,16,31}. The decoupling between FC and its structural basis is therefore thought to represent a key index of brain network pathology in psychiatric illnesses including schizophrenia^{15,45,46}. Our results are in line with the general notion that a structure-function breakdown in psychiatric illnesses involves anatomically defined hub brain regions¹⁴. The observed association with behavior, indicating that reduced structure-function coupling in feeder connections is related to higher severity of ADHD symptomology, provides support for the clinical relevance of this deficit in ADHD. By using a parsimonious model explaining the emergence of functional connectivity from underlying anatomical connectivity, we found that increased heteroscedasticity in intrinsic noise levels, either in hubs or periphery, has a strong detrimental effect in feeder connections, and to a lesser extent in hub-hub connections. Physiologically, reduced SC-FC coupling due to increased neural noise heteroscedasticity in peripheral regions can be understood as brain hubs being unable to average out peripheral functional disruptions. This adds weight to the notion that ADHD symptoms may arise from increased neural noise in the resting-state activity of associative brain regions^{19,20}. Our findings are also compatible with ADHD involving a deficit in catecholaminergic systems regulating neural signals (neural gain,¹⁷) and methylphenidate-induced reductions in neural noise^{19,47}.

Our empirical findings showed that feeder connections are the most affected by the decoupling between function and anatomy. Feeder connections comprise long-range anatomical routes allowing efficient communication between remote brain regions belonging to different brain networks²⁹. We here found that connections within control networks, as well as between regions comprising control and sensory networks, contributed to the overall reduction in structure-function association in ADHD. These findings are in agreement with previous neuroimaging studies in ADHD^{6,7,48,49} and healthy controls^{50,51}, highlighting the key role of these connectivity patterns to support normal and pathological attention and inhibitory processes. We also note that altered patterns of FC, and SC-FC decoupling, can occur in the absence of deficits in SC⁴⁵. In fact, whereas white matter connections are predictors of FC³¹, the opposite is not always true⁵².

The absence of significant group differences in the structural connectome is at odds with some previous reports^{3,4}. Due to the sample size and the quality of the data, it is unlikely that the negative finding reported here is due to a lack of statistical power in detecting meaningful differences in the ADHD connectome. Moreover, our result is consistent with recent work showing the existence of FC abnormalities with preserved white matter properties in ADHD⁵³. The discrepancy between our findings and earlier literature³ may be explained by non-neural factors. For example, the absence of significant differences between the ADHD

and control connectomes reported here may reflect our emphasis on comparable levels of head motion between the two groups; a critical factor that has recently been shown to produce spurious group differences in ADHD^{3,54}. Our cohort of medication-naive adults with established childhood-onset ADHD in the absence of co-occurring psychiatric conditions may also contribute to this negative finding, as psychostimulant exposure⁵⁵ and comorbidity⁵⁶ have been reported to affect SC in ADHD. Although our results cannot completely exclude the presence of altered white matter integrity in ADHD, they suggest that any such differences are small overall, and the manifestation of ADHD symptoms is underpinned by functional deregulations and related decoupling in SC-FC.

By combining functional and diffusion-weighted imaging with computational modeling, our study has advanced the understanding of neural mechanisms that underpin chronic ADHD symptoms. More specifically, our work showed that a clinically meaningful function-structure decoupling in ADHD is likely to be related to increased neural noise heterogeneity between hubs and periphery regions. This knowledge is consistent with the positive effect of current pharmacological interventions for ADHD and provides neurobiological support for future clinical research focusing on reducing periphery-to-hub noise amplitude ratio and peripheral noise heteroscedasticity using targeted interventions including brain stimulation.

Acknowledgments

This work was supported by the Ministry of Technology and Science, Taiwan (MOST103-2314-B-002-021-MY3), the National Health Research Institutes, Taiwan (NHRI-EX103-10008PI), and National Taiwan University Hospital (NTUH103-S2458, NTUH104-S2761). L.C. and J.A.R. are supported by the Australian National Health Medical Research Council (L.C., 1099082 and 1138711; J.A.R., 1145168 and 1144936).

Conflict of Interest

The authors declare no conflict of interest.

References

- 1 Asherson P, Buitelaar J, Faraone SV, Rohde LA. Adult attention-deficit hyperactivity disorder: key conceptual issues. *The Lancet Psychiatry* 2016; **3**: 568–578.
- 2 Sudre G, Mangalmurti A, Shaw P. Growing out of attention deficit hyperactivity disorder: Insights from the ‘remitted’ brain. *Neuroscience & Biobehavioral Reviews* 2018; **94**: 198–209.
- 3 Aoki Y, Cortese S, Castellanos FX. Research Review: Diffusion tensor imaging studies of attention-deficit/hyperactivity disorder: meta-analyses and reflections on head motion. *Journal of Child Psychology and Psychiatry* 2018; **59**: 193–202.
- 4 Chen L, Hu X, Ouyang L, He N, Liao Y, Liu Q *et al.* A systematic review and meta-analysis of tract-based spatial statistics studies regarding attention-deficit/hyperactivity disorder. *Neuroscience & Biobehavioral Reviews* 2016; **68**: 838–847.
- 5 van Ewijk H, Heslenfeld DJ, Zwiers MP, Buitelaar JK, Oosterlaan J. Diffusion tensor imaging in attention deficit/hyperactivity disorder: A systematic review and meta-analysis. *Neuroscience & Biobehavioral Reviews* 2012; **36**: 1093–1106.
- 6 Castellanos FX, Aoki Y. Intrinsic Functional Connectivity in Attention-Deficit/Hyperactivity Disorder: A Science in Development. *Biological Psychiatry: Cognitive Neuroscience and Neuroimaging* 2016; **1**: 253–261.
- 7 Cocchi L, Bramati IE, Zalesky A, Furukawa E, Fontenelle LF, Moll J *et al.* Altered Functional Brain Connectivity in a Non-Clinical Sample of Young Adults with Attention-Deficit/Hyperactivity Disorder. *J Neurosci* 2012; **32**: 17753–17761.
- 8 Samea F, Soluki S, Nejati V, Zarei M, Cortese S, Eickhoff SB *et al.* Brain alterations in children/adolescents with ADHD revisited: A neuroimaging meta-analysis of 96 structural and functional studies. *Neuroscience & Biobehavioral Reviews* 2019; **100**: 1–8.
- 9 Aoki Y, Yoncheva YN, Chen B, Nath T, Sharp D, Lazar M *et al.* Association of White Matter Structure With Autism Spectrum Disorder and Attention-Deficit/Hyperactivity Disorder. *JAMA Psychiatry* 2017; **74**: 1120–1128.
- 10 Rubia K, Alegria A, Brinson H. Imaging the ADHD brain: disorder-specificity, medication effects and clinical translation. *Expert Review of Neurotherapeutics* 2014; **14**: 519–538.
- 11 Lin H-Y, Cocchi L, Zalesky A, Lv J, Perry A, Tseng W-YI *et al.* Brain–behavior patterns define a dimensional biotype in medication-naïve adults with attention-deficit hyperactivity disorder. *Psychological Medicine* 2018; **48**: 2399–2408.
- 12 Deco G, Jirsa VK, McIntosh AR. Emerging concepts for the dynamical organization of resting-state activity in the brain. *Nature Reviews Neuroscience* 2011; **12**: 43–56.
- 13 Honey CJ, Kötter R, Breakspear M, Sporns O. Network structure of cerebral cortex shapes functional connectivity on multiple time scales. *PNAS* 2007; **104**: 10240–10245.
- 14 Crossley NA, Mechelli A, Scott J, Carletti F, Fox PT, McGuire P *et al.* The hubs of the human connectome are generally implicated in the anatomy of brain disorders. *Brain* 2014; **137**: 2382–2395.
- 15 van den Heuvel MP, Sporns O, Collin G, Scheewe T, Mandl RCW, Cahn W *et al.* Abnormal Rich Club Organization and Functional Brain Dynamics in Schizophrenia. *JAMA Psychiatry* 2013; **70**: 783.
- 16 Deco G, Kringelbach ML. Great Expectations: Using Whole-Brain Computational Connectomics for Understanding Neuropsychiatric Disorders. *Neuron* 2014; **84**: 892–905.

- 17 Hauser TU, Fiore VG, Moutoussis M, Dolan RJ. Computational Psychiatry of ADHD: Neural Gain Impairments across Marrian Levels of Analysis. *Trends in Neurosciences* 2016; **39**: 63–73.
- 18 Ziegler S, Pedersen ML, Mowinckel AM, Biele G. Modelling ADHD: A review of ADHD theories through their predictions for computational models of decision-making and reinforcement learning. *Neuroscience & Biobehavioral Reviews* 2016; **71**: 633–656.
- 19 Arnsten AFT. Catecholamine Influences on Dorsolateral Prefrontal Cortical Networks. *Biological Psychiatry* 2011; **69**: e89–e99.
- 20 Volkow ND, Fowler JS, Wang G-J, Telang F, Logan J, Wong C *et al*. Methylphenidate Decreased the Amount of Glucose Needed by the Brain to Perform a Cognitive Task. *PLOS ONE* 2008; **3**: e2017.
- 21 Kundu P, Inati SJ, Evans JW, Luh W-M, Bandettini PA. Differentiating BOLD and Non-BOLD Signals in fMRI Time Series Using Multi-Echo EPI. *Neuroimage* 2012; **60**: 1759–1770.
- 22 Chen Y-J, Lo Y-C, Hsu Y-C, Fan C-C, Hwang T-J, Liu C-M *et al*. Automatic whole brain tract-based analysis using predefined tracts in a diffusion spectrum imaging template and an accurate registration strategy. *Human Brain Mapping* 2015; **36**: 3441–3458.
- 23 Yeh F-C, Verstynen TD, Wang Y, Fernández-Miranda JC, Tseng W-YI. Deterministic Diffusion Fiber Tracking Improved by Quantitative Anisotropy. *PLOS ONE* 2013; **8**: e80713.
- 24 Yan C-G, Cheung B, Kelly C, Colcombe S, Craddock RC, Di Martino A *et al*. A Comprehensive Assessment of Regional Variation in the Impact of Head Micromovements on Functional Connectomics. *Neuroimage* 2013; **76**: 183–201.
- 25 Schaefer A, Kong R, Gordon EM, Laumann TO, Zuo X-N, Holmes AJ *et al*. Local-Global Parcellation of the Human Cerebral Cortex from Intrinsic Functional Connectivity MRI. *Cerebral Cortex* 2018; **28**: 3095–3114.
- 26 Hagmann P, Cammoun L, Gigandet X, Meuli R, Honey CJ, Wedeen VJ *et al*. Mapping the Structural Core of Human Cerebral Cortex. *PLoS Biol* 2008; **6**. doi:10.1371/journal.pbio.0060159.
- 27 Betzel RF, Byrge L, He Y, Goñi J, Zuo X-N, Sporns O. Changes in structural and functional connectivity among resting-state networks across the human lifespan. *NeuroImage* 2014; **102**: 345–357.
- 28 Perry A, Wen W, Lord A, Thalamuthu A, Roberts G, Mitchell PB *et al*. The organisation of the elderly connectome. *NeuroImage* 2015; **114**: 414–426.
- 29 Heuvel MP van den, Kahn RS, Goñi J, Sporns O. High-cost, high-capacity backbone for global brain communication. *PNAS* 2012; **109**: 11372–11377.
- 30 Van der Waerden B. Order tests for the two-sample problem and their power. Elsevier, 1952, pp 453–458.
- 31 Honey CJ, Sporns O, Cammoun L, Gigandet X, Thiran JP, Meuli R *et al*. Predicting human resting-state functional connectivity from structural connectivity. *Proc Natl Acad Sci U S A* 2009; **106**: 2035–2040.
- 32 Coghill D, Sonuga-Barke EJS. Annual Research Review: Categories versus dimensions in the classification and conceptualisation of child and adolescent mental disorders – implications of recent empirical study. *Journal of Child Psychology and Psychiatry* 2012; **53**: 469–489.

- 33 Demontis D, Walters RK, Martin J, Mattheisen M, Als TD, Agerbo E *et al.* Discovery of the first genome-wide significant risk loci for attention deficit/hyperactivity disorder. *Nature Genetics* 2019; **51**: 63.
- 34 Gau SS-F, Shang C-Y, Liu S-K, Lin C-H, Swanson JM, Liu Y-C *et al.* Psychometric properties of the Chinese version of the Swanson, Nolan, and Pelham, version IV scale – parent form. *International Journal of Methods in Psychiatric Research* 2008; **17**: 35–44.
- 35 Yeh C-B, Gau SS-F, Kessler RC, Wu Y-Y. Psychometric properties of the Chinese version of the adult ADHD Self-report Scale. *International Journal of Methods in Psychiatric Research* 2008; **17**: 45–54.
- 36 Zalesky A, Fornito A, Bullmore ET. Network-based statistic: identifying differences in brain networks. *Neuroimage* 2010; **53**: 1197–1207.
- 37 Barnett L, Buckley CL, Bullock S. Neural complexity and structural connectivity. *Physical Review E* 2009; **79**: 051914.
- 38 Deco G, Ponce-Alvarez A, Mantini D, Romani GL, Hagmann P, Corbetta M. Resting-State Functional Connectivity Emerges from Structurally and Dynamically Shaped Slow Linear Fluctuations. *Journal of Neuroscience* 2013; **33**: 11239–11252.
- 39 Saggio ML, Ritter P, Jirsa VK. Analytical Operations Relate Structural and Functional Connectivity in the Brain. *PLOS ONE* 2016; **11**: e0157292.
- 40 Friston KJ, Harrison L, Penny W. Dynamic causal modelling. *Neuroimage* 2003; **19**: 1273–1302.
- 41 Zalesky A, Fornito A, Cocchi L, Gollo LL, van den Heuvel MP, Breakspear M. Connectome sensitivity or specificity: which is more important? *Neuroimage* 2016; **142**: 407–420.
- 42 Shen X, Tokoglu F, Papademetris X, Constable RT. Groupwise whole-brain parcellation from resting-state fMRI data for network node identification. *Neuroimage* 2013; **82**: 403–415.
- 43 Fan L, Li H, Zhuo J, Zhang Y, Wang J, Chen L *et al.* The human brainnetome atlas: a new brain atlas based on connectional architecture. *Cerebral cortex* 2016; **26**: 3508–3526.
- 44 Gollo LL, Roberts JA, Cropley VL, Di Biase MA, Pantelis C, Zalesky A *et al.* Fragility and volatility of structural hubs in the human connectome. *Nature neuroscience* 2018; **21**: 1107.
- 45 Cocchi L, Harding IH, Lord A, Pantelis C, Yucel M, Zalesky A. Disruption of structure–function coupling in the schizophrenia connectome. *NeuroImage: Clinical* 2014; **4**: 779–787.
- 46 Skudlarski P, Jagannathan K, Anderson K, Stevens MC, Calhoun VD, Skudlarska BA *et al.* Brain connectivity is not only lower but different in schizophrenia: A combined anatomical and functional approach. *Biol Psychiatry* 2010; **68**: 61–69.
- 47 Engert V, Pruessner JC. Dopaminergic and noradrenergic contributions to functionality in ADHD: the role of methylphenidate. *Curr Neuropharmacol* 2008; **6**: 322–328.
- 48 Cary RP, Ray S, Grayson DS, Painter J, Carpenter S, Maron L *et al.* Network Structure among Brain Systems in Adult ADHD is Uniquely Modified by Stimulant Administration. *Cereb Cortex* 2017; **27**: 3970–3979.
- 49 Lin H-Y, Tseng W-YI, Lai M-C, Matsuo K, Gau SS-F. Altered Resting-State Frontoparietal Control Network in Children with Attention-Deficit/Hyperactivity Disorder. *Journal of the International Neuropsychological Society* 2015; **21**: 271–284.

- 50 Regev M, Simony E, Lee K, Tan KM, Chen J, Hasson U. Propagation of Information Along the Cortical Hierarchy as a Function of Attention While Reading and Listening to Stories. *Cereb Cortex* 2018. doi:10.1093/cercor/bhy282.
- 51 Weissman DH, Roberts KC, Visscher KM, Woldorff MG. The neural bases of momentary lapses in attention. *Nature Neuroscience* 2006; **9**: 971–978.
- 52 Stephan KE, Baldeweg T, Friston KJ. Synaptic Plasticity and Dysconnection in Schizophrenia. *Biological Psychiatry* 2006; **59**: 929–939.
- 53 Bos DJ, Oranje B, Achterberg M, Vlaskamp C, Ambrosino S, de Reus MA *et al.* Structural and functional connectivity in children and adolescents with and without attention deficit/hyperactivity disorder. *Journal of Child Psychology and Psychiatry* 2017; **58**: 810–818.
- 54 Yendiki A, Koldewyn K, Kakunoori S, Kanwisher N, Fischl B. Spurious group differences due to head motion in a diffusion MRI study. *NeuroImage* 2014; **88**: 79–90.
- 55 de Luis-García R, Cabús-Piñol G, Imaz-Roncero C, Argibay-Quiñones D, Barrio-Arranz G, Aja-Fernández S *et al.* Attention deficit/hyperactivity disorder and medication with stimulants in young children: A DTI study. *Progress in Neuro-Psychopharmacology and Biological Psychiatry* 2015; **57**: 176–184.
- 56 Adisetiyo V, Tabesh A, Martino AD, Falangola MF, Castellanos FX, Jensen JH *et al.* Attention-Deficit/Hyperactivity Disorder without Comorbidity is Associated with Distinct Atypical Patterns of Cerebral Microstructural Development. *Hum Brain Mapp* 2014; **35**: 2148–2162.
- 57 Allen M, Poggiali D, Whitaker K, Marshall TR, Kievit R. Raincloud plots: a multi-platform tool for robust data visualization. PeerJ Inc., 2018 doi:10.7287/peerj.preprints.27137v1.